ADVANCED OPTICAL MATERIALS

PATTERNING

On page 855, J. C. Ho and co-workers exploit a simple photolithographic technique using surface-textured soft polymer films as optical masks for the area selective exposure of photoresists upon flood UV illumination. This allows rapid fabrication of periodic nanopatterns over large areas, and by simply varying the mask and tuning the exposure dose, patterns with different geometric characteristics can be obtained in a controllable manner. Importantly, these polymer masks can be used numerous times, making this technique a reliable low-cost alternative to the existing methods.

WILEY-VCH

Optical Nanoscale Patterning Through Surface-Textured Polymer Films

*Ming Fang, Hao Lin, Ho-Yuen Cheung, SenPo Yip, Fei Xiu, Chun-Yuen Wong, and Johnny C. Ho**

In recent years, periodic nanostructure arrays have been extensively explored for widespread applications in areas such as photonics, plasmonics, photovoltaics, and biological/chemical sensors.[1–9] Generally, these nanostructures are fabricated via conventional lithographic techniques including deep-ultraviolet (UV), electron-beam, and focused ion-beam lithography; however, these techniques always encounter problems of either low patterning speed, small patterning area, or high equipment cost.[10] Substitutional and additive approaches consisting of nanoimprinting,[11] laser interference,[12] and epitaxy,[13,14] etc., have also been actively investigated, but they are still far from mature to be handled as standard methods. Lately, a low-cost patterning approach based on self-assembled nanospheres—nanosphere lithography (NSL)—has attracted tremendous attention and it has been employed for the construction of various periodic nanostructures such as nano-meshes, dots, disks, pillars, and cones.[5,15–19] Specifically, the anchored nanospheres would be used as obstacle masks for the subsequent patterning of thin films or for the etching of underlying structures. Wu et al. found that the dielectric nanospheres could also be utilized as optical masks/lenses for UV illumination to generate regular sub-wavelength patterns in photoresists, providing a new implementation for NSL.[20] At the same time, Chang et al. illustrated that the dielectric nanospheres could be further used to produce 3D photoresist nanostructures with designable lattice periods.[21] Nevertheless, in all these NSL-based approaches, the nanospheres are only used once and then sacrificed in the pattern-transfer procedures, leading to a high labor input and materials consumption as well as lowered controllability and reproducibility.

Here, we demonstrate a facile but reliable photolithographic technique, which allows the rapid fabrication of periodic nanopatterns by employing surface-textured soft polymer films as optical masks for the area-selective exposure of a photoresist upon flood UV illumination. Geometric characteristics of the obtained nanopattern can be controllably manipulated by varying the mask design, photoresist thickness, and exposure dose. Instead of a single usage, the polymer mask can be used numerous times without noticeable distortions in the achieved patterns. More importantly, the versatility of this lithographic approach can be validated with the fabrication of well-ordered nanoarrays of Au disks and rings, which support well surface plasmon oscillations, constituting an exciting platform for various technological applications, especially in the area of low-cost, label-free chemical- and bio-sensing.[22,23]

The process schematic of this newly developed photolithography technique is depicted in **Figure 1**, in which a flexible transparent polymer film surface textured with highly ordered micro-/nanohemispheres is used as the optical mask. The soft mask is first mounted on the photoresist layer with the textured side conformably in contact with the photoresist. The entire sample stack is then subjected to a flood UV illumination to perform an area-selective exposure and, after that, the soft mask is detached and the photoresist layer is developed to obtain the lithographically defined patterns. An obvious advantage of this method over the conventional NSL technique is that the polymer masks can be detached and repeatedly used, which makes the lithographic process much faster and more controllable. Also, this technique can be easily handled and does not involve any expensive equipment, so it could be highly accessible in the future as a generalized approach for the fabrication of nanopatterns.

Before the experimental development, finite difference time domain (FDTD) simulations were employed to assess the optical properties of the anchored micro-/nanohemispheres in order to guide the pattern design. In this work, we choose polydimethylsiloxane (PDMS) as the soft mask material due to its excellent optical transparency (from 240 to 1100 nm), elasticity, and tunable surface properties.[24] As shown in **Figure 2**, it is found that the PDMS hemispheres can indeed behave as microlenses to focus parallel UV light (365 nm) into tiny beams. Interestingly, when the diameter of the hemispheres is varied, the corresponding light propagation profiles become dramatically different. Specifically, when the diameter is as large as 1.2 μm, a central beam appears at ~110 nm below the contact interface, accompanied with a pair of symmetric beams at the shoulder. Along with the reduction in the diameter, the shoulder beams get weakened and finally disappear, meanwhile, the central beam gets upshifted. When the diameter is further shrunk to 0.6 μm, the light mainly converges at the mask–photoresist

M. Fang, H. Lin, S. P. Yip, F. Xiu, Prof. J. C. Ho
Department of Physics and Materials Science
and Centre for Functional Photonics (CFP)
City University of Hong Kong
83 Tat Chee Avenue
Kowloon, Hong Kong S.A.R., PR China
E-mail: johnnyho@cityu.edu.hk
H.-Y. Cheung, Prof. C.-Y. Wong
Department of Biology and Chemistry
City University of Hong Kong
83 Tat Chee Avenue
Kowloon, Hong Kong S.A.R., PR China
M. Fang, H. Lin, S. P. Yip, F. Xiu, Prof. J. C. Ho
Shenzhen Research Institute
City University of Hong Kong
Shenzhen, PR China

DOI: 10.1002/adom.201400127

© 2014 WILEY-VCH Verlag GmbH & Co. KGaA, Weinheim

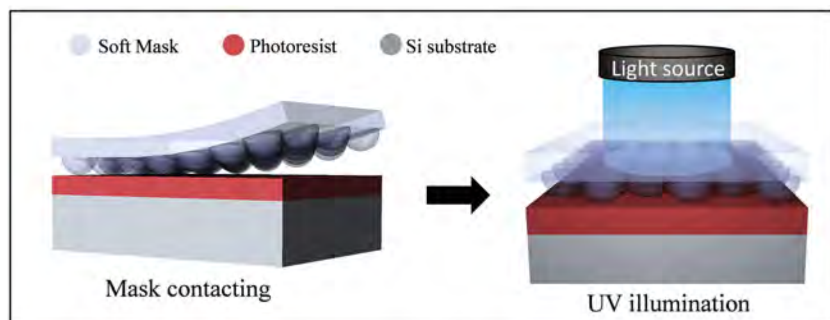

Figure 1. Schematic illustration of the soft-mask-assisted illumination in the lithography.

interface, which only allows the very thin photoresist layer (less than 230 nm) to be patterned. All these results confirm that it is possible to use a hemisphere-textured PDMS film as the optical mask for photolithography and the appropriate thickness of the photoresist is crucial to the success of this newly photolithographic technique.

In order to implement this soft mask-assisted photolithography, we first fabricated the masks via a double-casting approach by using self-assembled micro-/nanosphere monolayers as the starting templates, as illustrated in **Figure 3**a. Briefly, an inverted PDMS template was initially prepared by the casting and curing of liquid PDMS pre-polymers over a monolayer of self-assembled polystyrene (PS) nanoshperes on a silicon substrate. Notably, since the cured PDMS adhered strongly to the substrate but poorly to the PS nanospheres, this makes the necks among the nanospheres mechanical weak points; therefore, the PDMS layer would just delaminate at the plane along the dashed line (Figure 3a). The obtained inverted template was then treated with oxygen plasma and coated with a thin layer of Cu by sputtering, followed by a second casting and curing to fabricate the final soft mask with hemispheric textures. The Cu here serves as a release layer to ease the peeling-off of the second casing layer. Notably, other noble metals such as Au and Pt thin layers have also been used as the release layer in a previous report;[25] however, we found that these metals adhered poorly to PDMS and caused crumpled surfaces on the textured side owing to the significant mismatch of the thermal expansion coefficients (Supporting Information, Figure S1a). On the contrary, Cu, a nonprecious metal, was able to adhere well to the bottom plasma-treated PDMS layer and simultaneously offer a good peeling-off property to the top casting PDMS layer, giving the finished mask flat arranged surfaces (Supporting Information, Figure S1b). Also, the obtained mask displays a diffraction color (Figure 3b), indicating a long-range uniform distribution of surface textures over the soft mask surface. The corresponding morphology and microstructure were then further investigated utilizing a scanning electron microscope (SEM). Figure 3c, d, and e show typical SEM images of the starting PS sphere monolayer template, inverted PDMS template, and the final PDMS mask, respectively. The hemispheres on the mask are slightly rougher and smaller than the starting PS spheres owing to the utilization of the metal release layer; nevertheless, it still reveals the successful replication of the hemispheric structures.

The fabricated soft masks were next used to perform the area-selective exposure of photoresist layers. Before that, the texture side of the PDMS mask was treated with mild oxygen plasma to form a hardened shell of SiO_x which could prevent the defor-

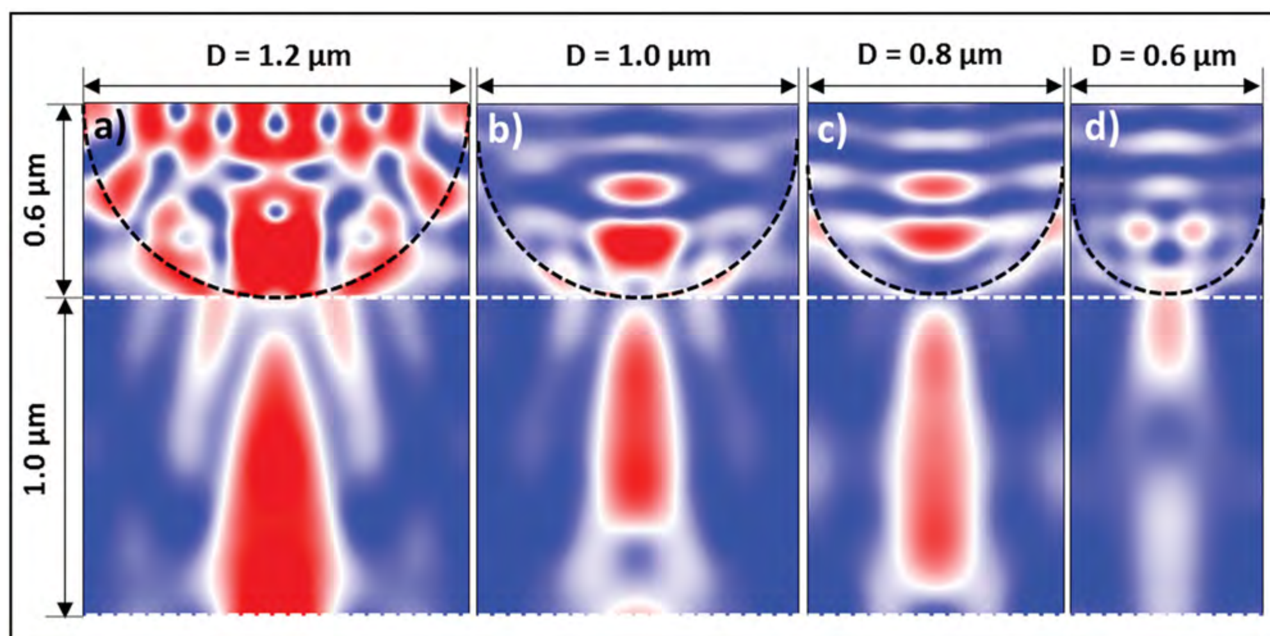

Figure 2. FDTD-calculated electric field distributions in photoresist layers underneath PDMS contacting masks with different hemisphere diameters. The black dashed arcs indicate the boarders of the PDMS masks while the white dashed lines signify the borders of photoresist layers, and the gaps between the black and white dashed lines are air.

© 2014 WILEY-VCH Verlag GmbH & Co. KGaA, Weinheim

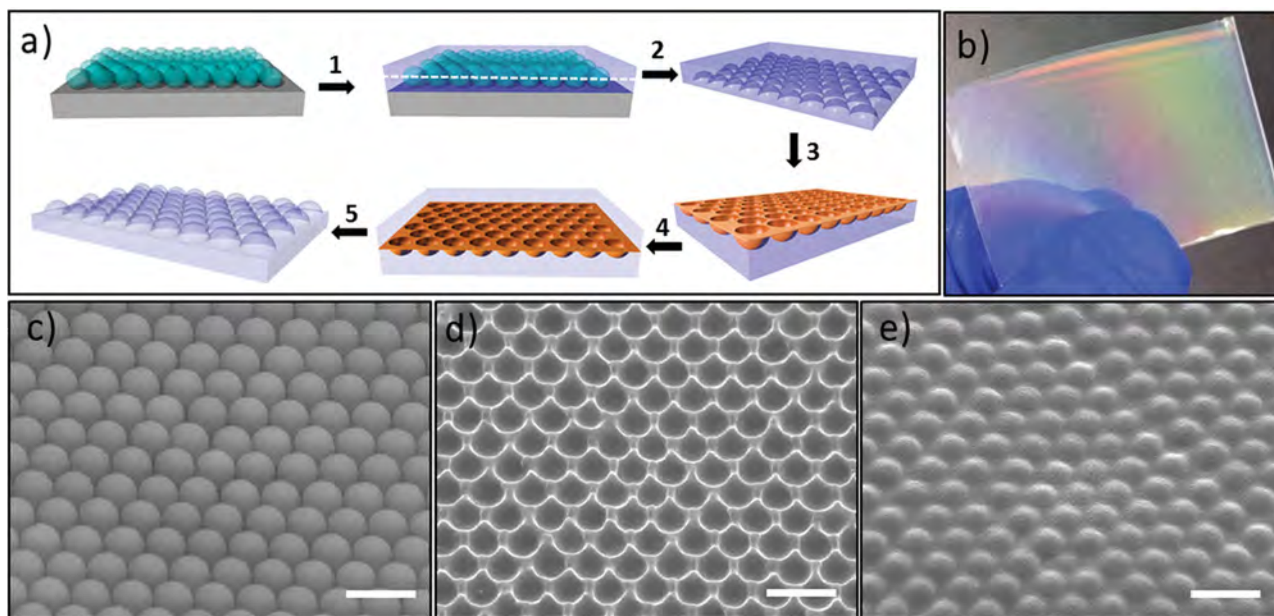

Figure 3. Fabrication of the PDMS soft masks. (a) Schematic illustration of the fabrication process. Step 1: PDMS casting on PS micro-/nanosphere monolayers; Step 2: top-layer peeled off after curing; Step 3: oxygen plasma treatment and copper coating (~30 nm thick by sputtering); Step 4: second PDMS casting; Step 5: peeling off the top layer to obtain the mask. (b) Photograph of the finished PDMS mask. (c–e) 45°-tilted-angle SEM images of self-assembled PS sphere monolayers, inversed PDMS templates obtained after Step 2 and the final PDMS mask, respectively. All scale bars are 2 μm.

mation of surface textures during contacting. The treated mask was then mounted on a photoresist layer to achieve a conformable contact. The lithographic process was conducted by successive UV flood illumination, mask detachment, and development. We first explored the lithography of thin photoresist layers (AZ5206E, ~450 nm) by employing a mask with a large hemisphere (1.2 μm in diameter) texture. By controlling the exposure and development time, three kinds of patterns were fabricated. With a short exposure time (2.5 s) and long development time (60 s), 'dot in hole' arrays are obtained (**Figure** 4a). Referring to Figure 2a, one can see that this special structure actually matches well with the simulation. Specifically, when the photoresist layer is thin, the light intensity at the center (in the vicinity of the contact interface) is weaker than that at the shoulders, which induces a circular exposure region in the photoresist and results a dot-in-hole pattern after the development. Meanwhile, we found that this kind of pattern could be transformed into other shapes by changing the exposure and development time. With a medium exposure and development time (3 s and 30 s, respectively), holes without dots in the sides were obtained (Figure 4b). Further increasing the exposure time to 4 s, the sidewalls of the holes shrank, leaving arrays of dots arranged in a hexagonal lattice (Figure 4c). Moreover, the mask was utilized to pattern thicker photoresist layers (AZ 5214E, ~1.0 μm). In this case, the pattern geometry was dominated by the central beam (Figure 2a), and thus we could obtain arrays of deep holes (Figure 4d) by thorough exposure and development of the photoresist layer. It is noted that the diameter of the holes here could be finely tuned by simply controlling the exposure time (Supporting Information, Figure S2). In order to further push down the structure size, soft masks made from 800 nm PS nanospheres were used for the lithography. Due to the excellent light-focusing effects of the soft mask, the obtained pattern shows well-defined hole structures. Figure 4e displays a typical SEM image of the patterned photoresist, showing an average hole diameter of ~385 nm, which could be precisely tuned between 250 and 470 nm by controlling the exposure time (Supporting Information, Figure S3). These results demonstrate that the geometric characteristics of the nanopattern can be manipulated by varying the mask design, photoresist thickness, and exposure dose. In most cases, they exhibit a relatively good uniformity in the obtained pattern with the statistical coefficient of variation (C_V, the ratio of the standard deviation to the mean) less than 5% (Figure S2, S3). More importantly, these masks are found to be quite robust for repeated usage, as no significant distortion or shape change was observed on either the mask or the obtained pattern after being used 50 times. All these results indicate that the soft mask-assisted photolithographic technique could be used as a versatile tool for the controllable fabrication of periodical nanopattern arrays.

In general, periodic nanostructures can find applications in various technological areas. For instance, highly ordered metallic nanostructures can support surface plasmon (SP) oscillations, providing exciting platforms for low-cost, label-free chemical-/bio-sensing, surface-enhanced infrared absorption (SEIRA), and surface-enhanced Raman scattering (SERS) applicaitons.[22,23,26,27] Using the photoresist patterns achieved by our soft mask-assisted photolithography, we can fabricate arrays of metallic nanostructures by vacuum thin-film deposition and subsequent lift-off. To facilitate the optical measurement, microscope glass slides were used as the substrates. Arrays of gold disks were constructed by utilizing photoresist patterns composed of holes, while rings were obtained through those containing 'dot-in-hole' patterns. **Figure 5** displays the extinction spectra and corresponding SEM images of three

© 2014 WILEY-VCH Verlag GmbH & Co. KGaA, Weinheim

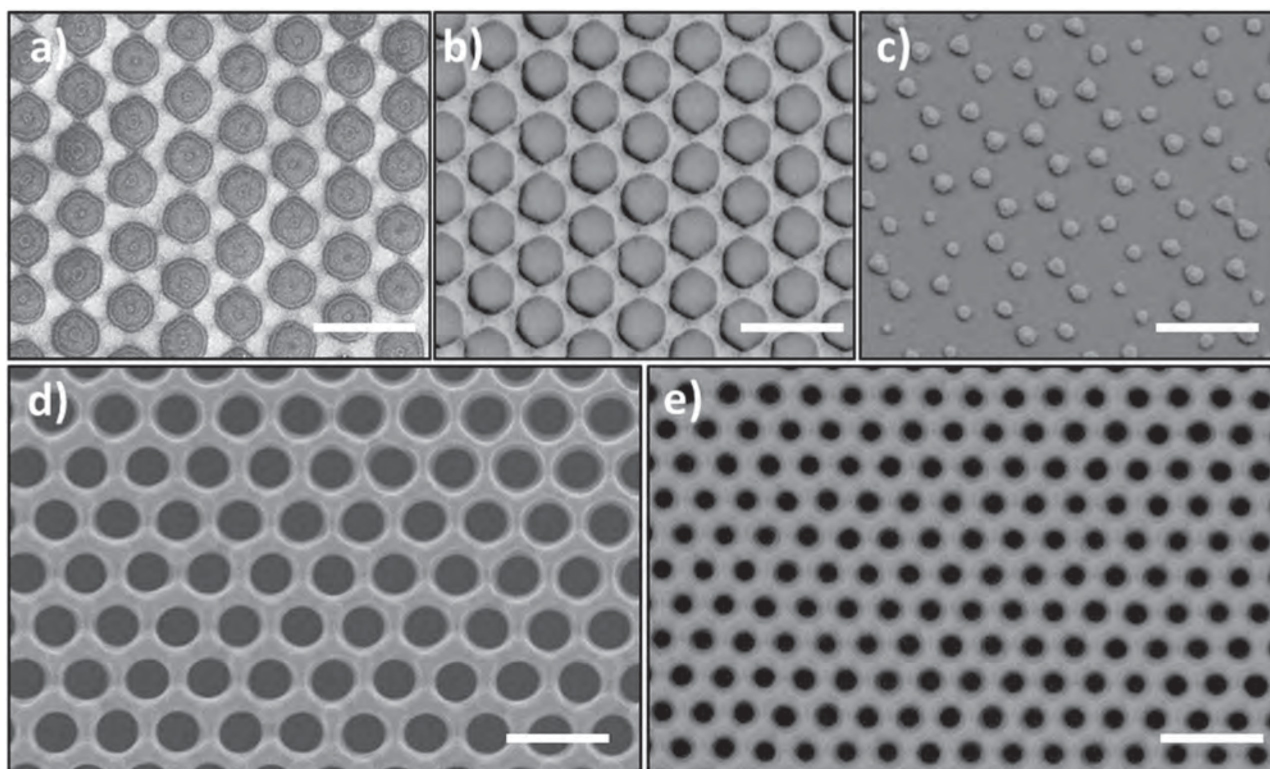

Figure 4. Representative SEM images of the photoresist patterns obtained with different experimental parameters. (a–d) Obtained with 1.2 μm hemisphere mask by using thin (a,b,c, AZ5206E) and thick photoresist layers (d,AZ5214E). (e) Obtained with 800 nm hemishpere mask and thin photoresist (AZ5206E). All scale bars are 2 μm.

different gold nanostructures with the same thickness (20 nm). Predominantly, the experimental measurements match well with the FDTD simulations, indicating a good uniformity of the gold nanopatterns. Also, as commonly observed in plasmonics,[28] the extinction spectra have a strong dependence on the size and geometry of the gold nanostructures. Notably, as these metal structures show a resonance effect at NIR and even extending to the mid-IR region (Figure 5c and Supporting Information Figure S4), they could be particularly interesting for the use of plasmonic biosensor elements as well as SEIRA substrates. Since our soft mask-assisted photolithography has illustrated its good capability to manipulate the particle size/shape, we can further fine-tune the structures to cater for more widespread applications.

In addition to 2D nanostrucurtres, periodical 3D nanostructures are also of great interest for various technical applicaitons. Previous studies show that PDMS phase masks could be used for 3D nanolithography,[29–31] and a recent report by Jeon et al.[32] demonstrated a similar technique by employing embedded colloidal particles as the phase mask. These stuides suggest that it is also possible to apply our lithographic method for 3D nanofabrication. Our preliminary simulation results (Supporting Information Figure S5) also support this assumption, which requires further experimental explorations.

In conclusion, a cost-effective and reliable soft mask-assisted photolithographic technique is presented for the facile fabrication of highly ordered micro-/nanopattern arrays. By simply varying the mask and tuning the exposure dose, patterns with different geometric characteristics could be obtained in a controllable manner. These patterns are further used as deposition masks to fabricate periodic metallic nanostructures, illustrating a geometry-dependent plasmonic effect. Obviously, this simple lithographic technique could be further optimized as a general approach for the viable large-area fabrication of periodic nanostructures, which could possibly boost the practical applications of nanostructures in a wide range, all the way from plasmonic sensors and multifunctional coatings to photovoltaics.

Experimental Section

Fabrications of PDMS Soft Masks: Masks surface-textured with hemisphere arrays were fabricated by a double-casting approach. First, close-packed monolayers of nanosphere arrays were prepared by self-assembly at the water–air interface and then transferred onto a silicon substrate. A mixture (1:10 by weight) of a curing agent and PDMS monomer (Sylgard 184, Dow Corning) was cast over the nanosphere assembly in a petri dish and baked on a hot plate at 60 °C for 2 h after degassing. The upper layer of the cured polymer was peeled off and used as the negative template for the final mask construction. Before the second PDMS casting, the negative template was flushed with acetone to remove any adhered PS nanospheres, then treated with oxygen plasma at 0.26 Torr with a power of 30 W for 30 s, and subsequently coated with a 30 nm-thick Cu layer by sputtering. The metal layer here behaves as a barrier to avoid merging of the two PDMS layers. After the second PDMS casting and curing, the upper PDMS layer (~1 mm in thickness) was peeled off, and treated with nitric acid solution to remove any metal debris (if needed). This upper layer was used as the final soft mask for photolithography.

© 2014 WILEY-VCH Verlag GmbH & Co. KGaA, Weinheim

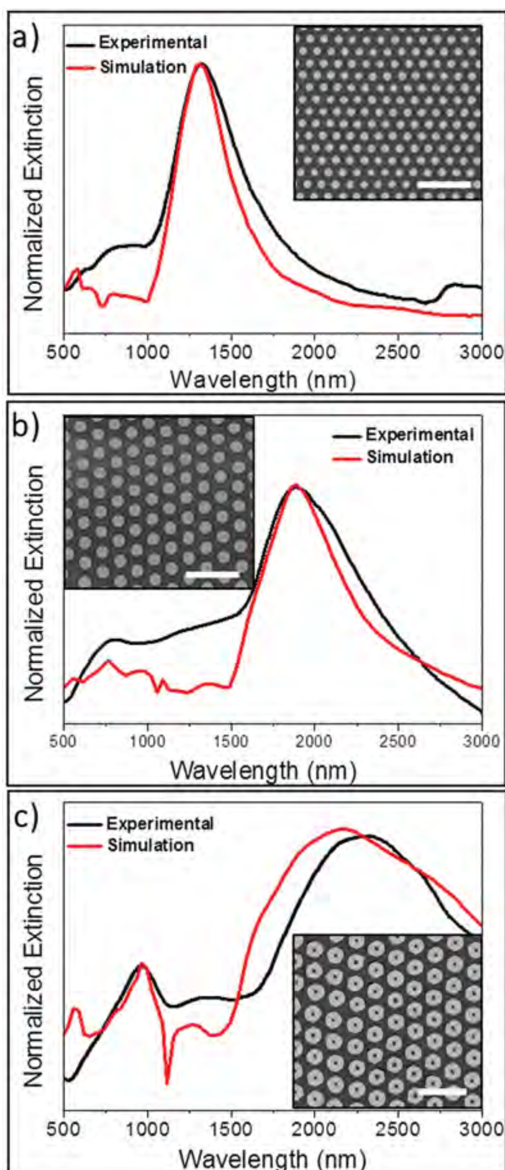

Figure 5. Experimental and calculated extinction spectra of different Au nanostructure arrays on glass substrates with the insets showing the corresponding SEM images. All scale bars in the SEM images are 3 μm.

Soft Mask-Assisted Photolithography: The photolithography was conducted in a class 100 clean room. Firstly, a layer of photoresist (AZ 5206E or AZ 5214E) was coated on a silicon wafer by spin coating and soft baking. The PDMS film was treated with oxygen plasma at 0.26 Torr with a power of 30 W for 30–60 s to form a thin, hardened SiO_x layer on the textured surface. The PDMS soft mask was put against the surface of the photoresist layer pre-deposited onto the substrate with gentle tapping to allow conformable contact. The sample was then illuminated by parallel UV light for a few seconds with a power intensity of 7.7 mWcm^{-2} at 365 nm via flood exposure in a SUSS MicroTec Mask Aligner. After the exposure, the soft mask was detached and reserved for subsequent reuse, and the exposed sample was developed in AZ-300 MIF developer, rinsed with DI water, and dried with nitrogen gas.

Fabrication of Metallic Nanostructures: The obtained photoresist patterns were used as masks for the metal deposition. A 2 nm thick Ti adhesion layer followed by a 20 nm thick Au layer were deposited by electron beam evaporation with a base pressure of 2.0×10^{-6} Torr at a rate of 1–2 Å/s. The samples were then immersed in acetone to lift off the photoresist and its bearing metal, rinsed with ethanol and dried with nitrogen gas.

FDTD Simulations: 3D FDTD simulations were performed using commercial software (FDTD solutions, Lumerical Solutions). A unit cell representing a hexagonal lattice with anti-symmetrical boundaries in the x-axis, symmetrical boundaries in the y-axis, and PML (perfectly matched layer) boundaries in the z-axis was set as the caculation region in each simulation, as illustrated in Figure S6 (Supporting Information). Also, we included a 0.6 μm-thick planar PDMS layer over the hemisphere region by assuming that the light is still parallel when achieving our simulating region. It is noted that, when compiling the figure, the entire simulation region was not included, for space-saving purposes. The refractive index of the PDMS and the photoresist were set as 1.4 and 1.69 at 365 nm (corresponding to the I-line of the mercury lamp used in the aligner), and the dielectric constants of the gold and glass were taken from Palik.[33] A plane-wave polarized parallel to the x-axis was used as the excitation source. The wavelength was set at 365 nm for the calculation the light profile in the photoresist (Figure 2) and at 400–3000 nm for the calculation of the extinction spectra of the gold nanostructures (Figure 5).

Supporting Information

Supporting Information is available from the Wiley Online Library or from the author. It includes optical images of the surface of PDMS masks fabricated by using different metal interfacial layer; SEM images and statistics of the photoresist pattern obtained using 1.2 μm and 800 nm hemisphere masks as well as thin photoresist layers (AZ5206E, 6000 rpm) with different exposure doses; an extended extinction spectrum (calculation) of the gold nanoring structure; FDTD-calculated electric field distributions in a 3 μm-thick photoresist layer, and; top view schematics of the unit cells employed in the FDTD simulations.

Acknowledgements

This research was supported by the Early Career Scheme of the Research Grants Council of Hong Kong SAR, China, under project number CityU139413, the National Natural Science Foundation of China (grant number 51202205), the Guangdong National Science Foundation (grant number S2012010010725), the Science Technology and Innovation Committee of Shenzhen Municipality (grant number JCYJ20120618140624228), and was supported by a grant from the Shenzhen Research Institute, City University of Hong Kong.

Received: March 20, 2014
Revised: May 2, 2014
Published online: May 26, 2014

[1] N. Yamada, R. Kojima, K. Hisada, T. Mihara, A. Tsuchino, N. Fujinoki, M. Birukawa, T. Matsunaga, N. Yasuda, Y. Fukuyama, K. Ito, Y. Tanaka, S. Kimura, M. Takata, *Adv. Optical Mater.* **2013**, *1*, 819.
[2] Z. A. Lewicka, Y. Li, A. Bohloul, W. W. Yu, V. L. Colvin, *Nanotechnology* **2013**, *24*, 115303.
[3] M. G. Deceglie, V. E. Ferry, A. P. Alivisatos, H. A. Atwater, *Nano Lett.* **2012**, *12*, 2894.
[4] Y. Lei, S. Yang, M. Wu, G. Wilde, *Chem. Soc. Rev.* **2011**, *40*, 1247.
[5] X. Ye, L. Qi, *Nano Today* **2011**, *6*, 608.
[6] L.-Y. Chen, Y.-Y. Huang, C.-H. Chang, Y.-H. Sun, Y.-W. Cheng, M.-Y. Ke, C.-P. Chen, J. Huang, *Opt. Express* **2010**, *18*, 7664.
[7] J. H. Moon, S. Yang, *Chem. Rev.* **2010**, *110*, 547.

© 2014 WILEY-VCH Verlag GmbH & Co. KGaA, Weinheim

[8] R. Yerushalmi, J. C. Ho, Z. A. Jacabson, A. Javey, *Nano Lett.* **2007**, *7*, 2764.
[9] J. Henzie, J. E. Barton, C. L. Stender, T. W. Odom, *Acc. Chem. Res.* **2006**, *39*, 249.
[10] B. D. Gates, Q. Xu, M. Stewart, D. Ryan, C. G. Willson, G. M. Whitesides, *Chem. Rev.* **2005**, *105*, 1171.
[11] L. J. Guo, *Adv. Mater.* **2007**, *19*, 495.
[12] Q. Xie, M. H. Hong, H. L. Tan, G. X. Chen, L. P. Shi, T. C. Chong, *J. Alloys Compd.* **2008**, *449*, 261.
[13] J. J. Hou, N. Han, F. Wang, F. Xiu, S. Yip, A. T. Hui, T. Hung, J. C. Ho, *ACS Nano* **2012**, *6*, 3624.
[14] N. Han, F. Y. Wang, A. T. Hui, J. J. Hou, G. C. Shan, F. Xiu, T. F. Hung, J. C. Ho, *Nanotechnology* **2011**, *22*, 285607.
[15] J. Hulteen, R. Van Duyne, *J. Vac. Sci. Technol. A* **1995**, *13*, 1553.
[16] C. Haynes, R. Van Duyne, *J. Phys. Chem. B* **2001**, *105*, 5599.
[17] A. Kosiorek, W. Kandulski, H. Glaczynska, M. Giersig, *Small* **2005**, *1*, 439.
[18] H. Lin, F. Xiu, M. Fang, S. P. Yip, H.-Y. Cheung, F. Y. Wang, N. Han, K. S. Chan, C.-Y. Wong, J. C. Ho, *ACS Nano* **2014**, *8*, 3752.
[19] H. Lin, H.-Y. Cheung, F. Xiu, F. Wang, S. Yip, N. Han, T. Hung, J. Zhou, J. C. Ho, C.-Y. Wong, *J. Mater. Chem. A* **2013**, *1*, 9942.
[20] W. Wu, A. Katsnelson, O. G. Memis, H. Mohseni, *Nanotechnology* **2007**, *18*, 485302.
[21] C.-H. Chang, L. Tian, W. R. Hesse, H. Gao, H. J. Choi, J.-G. Kim, M. Siddiqui, G. Barbastathis, *Nano Lett.* **2011**, *11*, 2533.
[22] K. M. Mayer, J. H. Hafner, *Chem. Rev.* **2011**, *111*, 3828.
[23] C. Valsecchi, A. G. Brolo, *Langmuir* **2013**, *29*, 5638.
[24] J. C. McDonald, G. M. Whitesides, *Acc. Chem. Res.* **2002**, *35*, 491.
[25] H. Hassanin, A. Mohammadkhani, K. Jiang, *Lab Chip* **2012**, *12*, 4160.
[26] H. Im, K. C. Bantz, S. H. Lee, T. W. Johnson, C. L. Haynes, S.-H. Oh, *Adv. Mater.* **2013**, *25*, 2678.
[27] X. A. Zhang, J. Elek, C.-H. Chang, *ACS Nano* **2013**, *7*, 6212.
[28] Y. Sonnefraud, a. Leen Koh, D. W. McComb, S. a. Maier, *Laser Photon. Rev.* **2012**, *6*, 277.
[29] S. Jeon, J.-U. Park, R. Cirelli, S. Yang, C. E. Heitzman, P. V Braun, P. J. A. Kenis, J. A. Rogers, *Proc. Natl. Acad. Sci. USA* **2004**, *101*, 12428.
[30] X. A. Zhang, J. Elek, C.-H. Chang, *ACS Nano* **2013**, *7*, 6212.
[31] J.-W. Jang, Z. Zheng, O.-S. Lee, W. Shim, G. Zheng, G. C. Schatz, C. A. Mirkin, *Nano Lett.* **2010**, *10*, 4399.
[32] T. Y. Jeon, H. C. Jeon, S. Y. Lee, T. S. Shim, J.-D. Kwon, S.-G. Park, S.-M. Yang, *Adv. Mater.* **2014**, *26*, 1422.
[33] E. Palik, *Handbook of Optical Constants of Solids*, Academic Press, San Diego, CA **1998**.

© 2014 WILEY-VCH Verlag GmbH & Co. KGaA, Weinheim